J|A|C|S ARTICLES

Published on Web 02/12/2009

Spin Glass Behavior of Isolated, Geometrically Frustrated Tetrahedra of Iron Atoms in the Intermetallic $La_{21}Fe_8Sn_7C_{12}$

Evan M. Benbow, Naresh S. Dalal, and Susan E. Latturner*

Department of Chemistry and Biochemistry, Florida State University, Tallahassee, Florida 32306

Received November 19, 2008; E-mail: latturne@chem.fsu.edu

Abstract: Metal flux synthesis in a low-melting eutectic mixture of lanthanum and nickel has produced a family of complex intermetallic carbide phases. $La_{21}Fe_8M_7C_{12}$ (M = Sn, Bi, Sb, Te, Ge) has a new cubic structure featuring tetrahedra of iron atoms capped with carbon on each edge. These tetrahedra are surrounded by a La/M framework and are therefore isolated from each other. The antiferromagnetic coupling of the iron atoms is frustrated by their ideal tetrahedral arrangement; this is evidenced by magnetic susceptibility measurements on the $La_{21}Fe_8Sn_7C_{12}$ analogue. Deviations from Curie−Weiss behavior begin at 100 K; variation in field-cooled vs zero-field-cooled behavior is seen at 5 K indicative of magnetic ordering. AC susceptibility data indicate that the temperature of this transition is frequency-dependent, behavior characteristic of spin glass systems.

Introduction

Relatively few metallic carbides have been discovered in comparison to the large number of intermetallics containing other main group elements, such as aluminum and silicon, which have been investigated for their unique electronic and physical properties. Carbide phases are typically known for their hardness (e.g., tungsten carbide and steel), but complex carbides such as Y_2FeC_4 and $LaNi_2B_2C$ also display superconductivity, with the latter displaying an unusual relationship between superconductivity and magnetism.[1,2] Pöttgen and Jeitschko et al. have discovered many of the known inorganic carbides. These phases often contain isolated carbon atoms (C_1), although some feature C_2 and C_3 units; the highly complex unit cell of Sc_3C_4 features 12 C_1, 2 C_2, and 8 C_3 units.[3] Exploratory synthesis of carbide phases increases the probability of discovering compounds with interesting physical properties featuring carbon in unique environments.

We are investigating molten metal solvents (flux) as growth media in an effort to synthesize new carbide intermetallic compounds. Metal flux synthesis has proven to be a very useful technique for isolating a variety of intermetallic phases.[4] Carbon is usually not reactive in commonly used flux metals, such as tin and indium, so more aggressive fluxes are being explored. Due to their high melting points, lanthanum (mp 918 °C) and nickel (mp 1455 °C) are usually not considered suitable solvents for flux chemistry. However, when combined in an 88:12 wt % ratio, they form a eutectic with a melting point of 532 °C.[5] Our efforts in using this mixture for synthesis of intermetallics have yielded crystals of many interesting phases, such as $La_6T_{13-x}Al_{1+x}$ (T = Fe, Mn), $LaFe_{12}B_6$, and $La_{3.67}FeC_6$, in addition to the novel carbide phases $La_{21}Fe_8M_7C_{12}$ (M = Bi, Sb, Sn, Te, Ge).[6−8] The title compounds have a new cubic structure type that features isolated tetrahedra of iron atoms edge-capped by carbon in a network of La/M, as shown in Figure 1.

Isolated tetrahedra of magnetic atoms or ions with equal antiferromagnetic coupling constants J_{ij} are of interest as examples of ideal spin-frustrated units. However, due to the lack of real-world compounds possessing such building blocks, they are referred to as "toy problems" by the theoretical and computational researchers studying them.[9,10] The analogous 2-D toy problem of nets or chains of equilateral triangles of magnetic ions is roughly approximated by the kagome lattice of jarosites and olivines, some of which have been found to show characteristic signs of spin frustration.[11,12] Compounds containing structural units that approximate the ideal tetrahedral arrangements of magnetic atoms which are associated with geometric frustration include the cubic pyrochlore structure

(1) Gerss, M. H.; Jeitschko, W.; Boonk, L.; Nientiedt, J.; Grobe, J.; Mörsen, E.; Leson, A. *J. Solid State Chem.* **1987**, *70*, 19–28.
(2) Canfield, P. C.; Gammel, P. L.; Bishop, D. J. *Physics Today* **1998**, 40.
(3) (a) Pöttgen, R.; Jeitschko, W. *Inorg. Chem.* **1991**, *30*, 427–431. (b) Hoffmann, R. *Am. Sci.* **2002**, *90*, 318–320.
(4) (a) Kanatzidis, M. G.; Pöttgen, R.; Jeitschko, W. *Angew. Chem., Int. Ed.* **2005**, *44*, 6996–7023. (b) Stojanovic, M.; Latturner, S. E. *J. Solid State Chem.* **2007**, *180*, 907–914.
(5) Massalski, T. B.; Okamoto, H. *Binary Alloy Phase Diagrams*, 2nd ed.; ASM International: Materials Park, OH, 1990.
(6) (a) Benbow, E. M.; Latturner, S. E., in preparation. (b) Benbow, E. M. Ph.D. Dissertation, Florida State University, 2008.
(7) Rosenberg, M.; Sinnemann, T.; Mittag, M.; Buschow, K. H. J. *J. Alloys Compd.* **1992**, *182*, 145.
(8) Witte, A. M.; Jeitschko, W. *Z. Naturforsch. B: Chem. Sci.* **1996**, *51*, 249.
(9) Saunders, T. E.; Chalker, J. T. *Phys. Rev. Lett.* **2007**, *98*, 157201(4).
(10) Bellier-Castella, L.; Gingras, M. J. P.; Holdsworth, P. C. W.; Moessner, R. *Can. J. Phys.* **2001**, *79*, 1365–1371.
(11) Hagemann, I. S.; Khalifah, P. G.; Ramirez, A. P.; Cava, R. J. *Phys. Rev. B* **2000**, *62*, R771–774.
(12) (a) Shores, M. P.; Nytko, E. A.; Bartlett, B. M.; Nocera, D. G. *J. Am. Chem. Soc.* **2005**, *127*, 13462–13463. (b) Bartlett, B. M.; Nocera, D. G. *J. Am. Chem. Soc.* **2005**, *127*, 8985–8993.

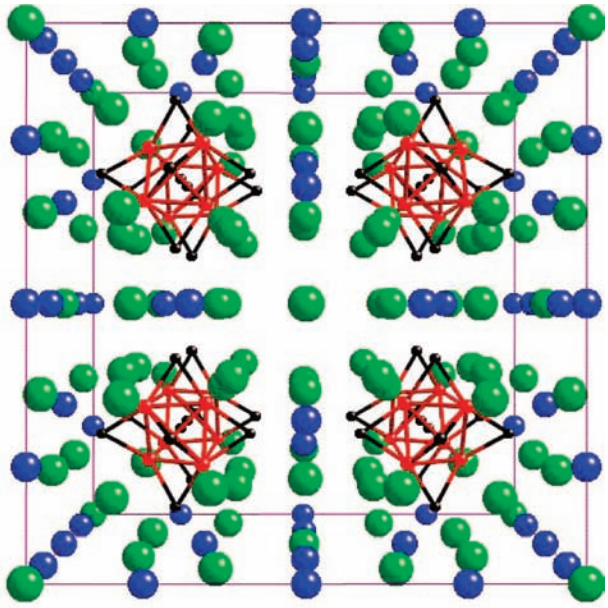

Figure 1. Cubic structure of $La_{21}Fe_8M_7C_{12}$. Green and blue spheres represent lanthanum and M atoms, respectively. The Fe_4C_6 tetrahedral clusters are represented in red and black.

($A_2B_2O_7$), such as $Mn_2Sb_2O_7$.[13] This pyrochlore structure features a 3-D network of corner-sharing Mn^{2+} tetrahedra with interesting ground states without long-range magnetic order, resulting in complex magnetic states such as spin glasses, spin ices, and spin liquids.[14] Conventional spin glasses are commonly described using randomness (disorder in the location of magnetic ions) and competing exchange interactions; however, some pyrochlores without apparent structural disorder display spin glass ordering with ground states that are not well defined either experimentally or theoretically.[15] Investigations into the properties of an isolated tetrahedron of magnetic ions could provide useful information for the understanding of materials possessing geometric frustration with little possibility for long-range magnetic ordering. To this end, single crystals of the cubic $La_{21}Fe_8Sn_7C_{12}$ have been characterized by means of SEM-EDS, X-ray diffraction, and SQUID magnetometry (both DC and AC). The magnetic properties deviate from Curie−Weiss behavior below 130 K, with a spin glass transition (T_{SG}) observed below 5 K.

Experimental Section

Synthesis. Starting materials were powders of lanthanum (MET-ALL Rare Earth Ltd. or Acros, purity >99.9%), powders/chips of Fe, Bi, Sb, Sn, Ge, or Te (Strem Chemicals, 99.9%), carbon in the form of acetylene carbon black (Strem Chemicals, 99.99%), and chips ground from ingots of commercially available La/Ni eutectic (88:12 wt %, Alfa Aesar 99.9%). The $La_{21}Fe_8Sn_7C_{12}$ phase was originally grown in a synthesis mixture of 1 mmol of Fe, 2 mmol of C, and 1 mmol of Sn in 1 g of La/Ni flux. After determining the structure, it was found that these compounds are optimally synthesized from a stoichiometric ratio of the component elements (for example, 2.1 mmol of La, 0.8 mmol of Fe, 0.7 mmol of Sn, 1.2 mmol of C) sandwiched between layers of La/Ni eutectic (~1.2 g total) in an alumina crucible sealed in a fused silica tube under vacuum of 10^{-2} Torr. In addition to the alumina crucible containing the reactants, another alumina crucible was filled with Fiberfrax and inverted above the reaction crucible in the silica tube to act as a filter during centrifugation. The fused silica ampule was then heated to 950 °C in 3 h, held at this temperature for 12 h, and then cooled to 850 °C in 10 h. The reaction mixtures were subsequently annealed for 48 h at 850 °C and then cooled to 600 °C in 84 h. At 600 °C the fused silica ampules were removed from the furnace, quickly inverted, and placed into a centrifuge to remove excess molten flux. Any flux remaining on the surface of the product can be removed mechanically or by briefly leaving the crystals in air to preferentially oxidize the La-rich flux coating. Products were then kept in a drybox to prevent any further oxidation. The $La_{21}Fe_8M_7C_{12}$ crystals are stable enough in air to allow overnight X-ray collections under ambient conditions, but they will degrade if left in air for longer periods.

Stoichiometric synthesis of $La_{21}Fe_8Sn_7C_{12}$ was attempted by arc-melting a mixture of the elements under argon on a water-cooled copper hearth. The La, Fe, and C reactant powders were mixed in a stoichiometric ratio and wrapped in a stoichiometrically appropriate mass of tin foil before arc-melting to prevent the volatilization of the powdered reactants. The resulting reaction pellet was flipped and arc-melted several times to ensure homogeneity. The pellet was then placed in an alumina crucible and sealed in a fused silica tube to be annealed at 800 °C for two weeks. Powder X-ray diffraction (using a Rigaku Ultima III rotating anode source CCD diffractometer) was used to determine the phase purity of the arc-melted pellet. Diffraction peaks corresponding to the title phase were dominant in the powder pattern, but additional peaks indicate a number of secondary phases were also formed. It was not possible to isolate a pure sample of $La_{21}Fe_8Sn_7C_{12}$ using stoichiometric synthesis.

Elemental Analysis. Elemental analysis was performed on all samples using a JEOL 5900 scanning electron microscope with energy-dispersive spectroscopy (SEM-EDS) capabilities. Samples were analyzed using a 30 kV accelerating voltage and an accumulation time of 40 s. Scans of the surface and interiors of cleaved crystals typically showed molar ratios for La, Fe, and M of 20:8:8. Stoichiometric values could not be resolved for carbon due to the limitation of EDS with light elements ($Z < 11$). Traces of aluminum were observed in the M = Ge and Te analogues. Because of the possibility of Ni contamination from the flux, the samples were also monitored for this element; it was evident on the surface but not in any of the scans of the interior of the crystals.

X-ray Diffraction. Small shards were cleaved from the interior of large flux-grown single crystals of $RE_{21}Fe_8M_7C_{12}$ previously analyzed by EDS. The shards were mounted on glass fibers using epoxy, and single-crystal X-ray diffraction data for each compound were collected at room temperature on a Bruker AXS SMART CCD diffractometer. Frame exposure times of 10 s were usually sufficient. Data processing was then performed using the program SAINT; an adsorption correction was applied to the data using the SADABS program. The structure was solved using direct methods and refined with the SHELXTL package of programs.[16] For most of the analogues, it was necessary to refine the carbon atoms isotropically. During the final refinement cycles, occupancies of all sites were allowed to vary, and lowered electron density was indicated on the 24*e* site for the Te and Ge analogues. Since aluminum impurities were indicated by the EDS analysis of these analogues, aluminum was allowed to mix on this site. Details of the single-crystal data collection of one of the analogues ($La_{21}Fe_8Sn_7C_{12}$) are listed in Table 1; further crystallographic information for all analogues can be found in the Supporting Information.

Magnetic Susceptibility. Magnetic susceptibility measurements were performed with a Quantum Design MPMS SQUID magnetometer on single crystals (previously analyzed by EDS; total mass

(13) Zhou, H. D.; Wiebe, C. R.; Harter, A.; Dalal, N. S.; Gardner, J. S. *J. Phys.: Condens. Matter.* **2008**, *20*, 325201.
(14) Greedan, J. E. *J. Mater. Chem.* **2001**, *11*, 37–53.
(15) Gingras, M. J. P.; Stager, C. V.; Raju, N. P.; Gaulin, B. D.; Greedan, J. E. *Phys. Rev. Lett.* **1997**, *78*, 947–950.
(16) (a) *SAINT*, version 6.02a; Bruker AXS Inc.: Madison WI, 2000. (b) Sheldrick, G. M. *SHELXTL NT/2000*, version 6.1; Bruker AXS, Inc.: Madison, WI, 2000.

Table 1. Crystallographic Data Collection Parameters for $La_{21}Fe_8Sn_7C_{12}$

empirical formula	$La_{21}Fe_8Sn_7C_{12}$
formula weight (g/mol)	4338.86
space group	$Fm\bar{3}m$ (No. 225)
a (Å)	16.6032(4)
V (Å^3)	4576.94(19)
d_{calc} (g/cm^3)	6.297
Z	4
temperature (K)	298
radiation	Mo Kα
$2\theta_{max}$	56.43
index ranges	$-22 \le h, k, l \le 22$
reflections collected	15 699
unique data/parameters	337/21
μ (mm^{-1})	25.28
R_1/wR_2[a] [$I > 2\sigma(I)$]	0.0233/0.0533
R_1/wR_2 (all data)	0.0233/0.0533
residual peaks/hole (e/Å^3)	3.22/−1.18

[a] $R_1 = \sum||F_o| - |F_c||/\sum|F_o|$; $wR_2 = [\sum[w(F_o^2 - F_c^2)^2]/\sum[w(F_o^2)^2]]^{1/2}$.

8.2 mg) sealed in kapton tape. DC susceptibility measurements were performed at temperatures between 1.8 and 300 K; field-cooled (FC) and zero-field-cooled (ZFC) temperature dependence measurements were collected at various fields, with field-dependent measurements collected at 1.8K. AC susceptibility data were collected from 1.8 to 10 K, with an applied field of 5 Oe at four different frequencies.

Results and Discussion

La/Ni eutectic flux has proven to be a rich synthesis medium for crystal growth of complex intermetallic phases. This flux is an unusual combination of a reactive element (lanthanum, always incorporated into the product) and a component that is inert under certain conditions (nickel). In the absence of iron, nickel-containing products are crystallized, including $La_5Ni_{2-d}Si_3$, La_5Ni_2Sn (Cr_5B_3 structure type), and LaNiAl.[17] However, if iron is present in the reaction mixture, nickel from the flux is not incorporated into products. This allows for the isolation of a variety of La/Fe/X (X = C, B, Al, C, Sn, etc.) multinary intermetallic phases from these reactions, without having to use the much higher melting La/Fe eutectic as a solvent. For the $La_{21}Fe_8M_7C_{12}$ title compounds, well-faceted spheroid crystals of up to 1 mm on a side can be grown in La/Ni flux; an example is shown in Figure 2. The phase diagrams of other early rare earth (RE) elements with nickel or iron possess similar eutectics in the RE-rich region; use of these mixtures as fluxes leads to analogues containing other rare earths. For instance, $Ce_{21}Fe_8Bi_7C_{12}$ can be synthesized from the reaction of C and Bi in the Ce/Fe eutectic at 92.6 wt % Ce (mp 592 °C). The eutectic fluxes used are aggressive enough reducing agents to leach Al from the alumina crucible; this can be limited by utilizing an initial soak temperature of 950 °C with a short soak (6 h). The crystallographic parameters of several $RE_{21}Fe_8M_7C_{12}$ analogues have been determined by single-crystal X-ray diffraction; the unit cells and R-values are listed in Table 2.

Structural Description. The structure of $La_{21}Fe_8M_7C_{12}$ is shown in Figure 1; it features isolated iron tetrahedra edge-capped by carbon in an extended La/M network. Although the La can be substituted by other early rare earth elements Ce and Pr, and analogues can be made with M = Sn, Bi, Sb, Te, and Ge, only the $La_{21}Fe_8Sn_7C_{12}$ analogue will be discussed; its atomic positions and bond lengths are presented in Tables 3 and 4. This structure occupies an odd position in the classification of metallic carbides. A survey by Jeitschko divided these materials into two classes.[18] The "carbometallates" are line compounds with an electropositive metal balancing the charge

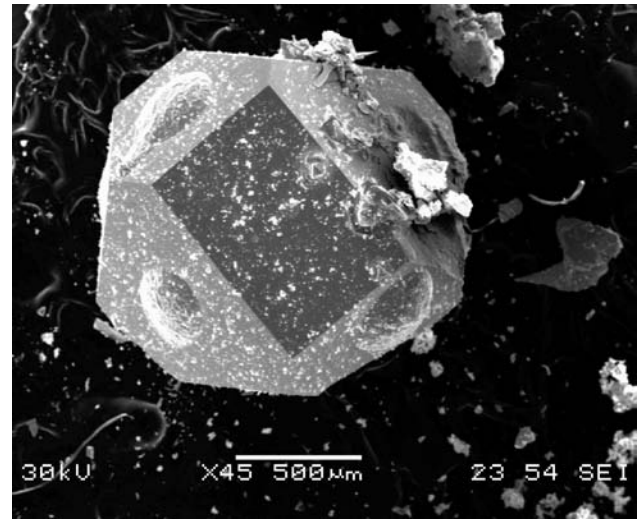

Figure 2. SEM image of a flux-grown crystal of $La_{21}Fe_8Sn_7C_{12}$. Droplets of excess La/Ni flux are seen flaking off the faceted crystal.

Table 2. Unit Cell Parameters and R-Values ($I > 2\sigma(I)$) for $RE_{21}Fe_8M_7C_{12}$ Analogues

compound	a (Å)	R_1/wR_2
$La_{21}Fe_8Sn_7C_{12}$	16.6032(4)	0.0233/0.0533
$La_{21}Fe_8Sb_7C_{12}$	16.4101(2)	0.0281/0.0668
$La_{21}Fe_8Te_{4.2}Al_{2.8}C_{12}$	16.2911(7)	0.0422/0.0947
$La_{21}Fe_8Ge_{4.9}Al_{2.1}C_{12}$	16.1589(4)	0.0208/0.0483
$La_{21}Fe_8Bi_7C_{12}$	16.4863(5)	0.0326/0.0692
$Ce_{21}Fe_8Bi_7C_{12}$	16.2992(3)	0.0243/0.0483
$Pr_{21}Fe_8Bi_7C_{12}$	16.2124(5)	0.0258/0.0582

Table 3. Atomic Coordinates and Equivalent Isotropic Displacement Parameters for $La_{21}Fe_8Sn_7C_{12}$

atom	Wyckoff site	x	y	z	U_{eq}[a]
La1	48h	0	0.16989(3)	y	0.0091(2)
La2	32f	0.36500(3)	x	x	0.0080(2)
La3	4b	1/2	1/2	1/2	0.0169(6)
Fe	32f	0.19561(8)	x	x	0.0088(4)
Sn1	24e	0.28894(8)	0	0	0.0096(3)
Sn2	4a	0	0	0	0.0102(6)
C	48g	0.1096(9)	1/4	1/4	0.014(2)

[a] U_{eq} is defined as the trace of the orthogonalized U_{ij} tensor.

Table 4. Selected Bond Distances for $La_{21}Fe_8Sn_7C_{12}$

bond	length (Å)
La−La	3.7620(15)−3.9891(7)
Sn1−La1	3.4444(8) × 4
Sn1−La2	3.4122(7) × 4
Sn1−La3	3.5042(13) × 1
Sn2−La1	3.9891(1) × 12
Fe1−Fe1	2.554(4) × 3
Fe1−C1	1.915(11) × 3
Fe1−La1	3.3033(17) × 3
Fe1−La2	3.1520(9) × 3
C1−La1	2.618(10) × 2
C1−La2	2.733(2) × 2

(17) Villars, P.; Calvert, L. D. *Pearson's Handbook—Crystallographic Data for Intermetallic Phases*; ASM International: Materials Park, OH, 1998.

(18) Dashjav, E.; Kreiner, G.; Schnelle, W.; Wagner, F. R.; Kniep, R.; Jeitschko, W. *J. Solid State Chem.* **2007**, *180*, 636–653.

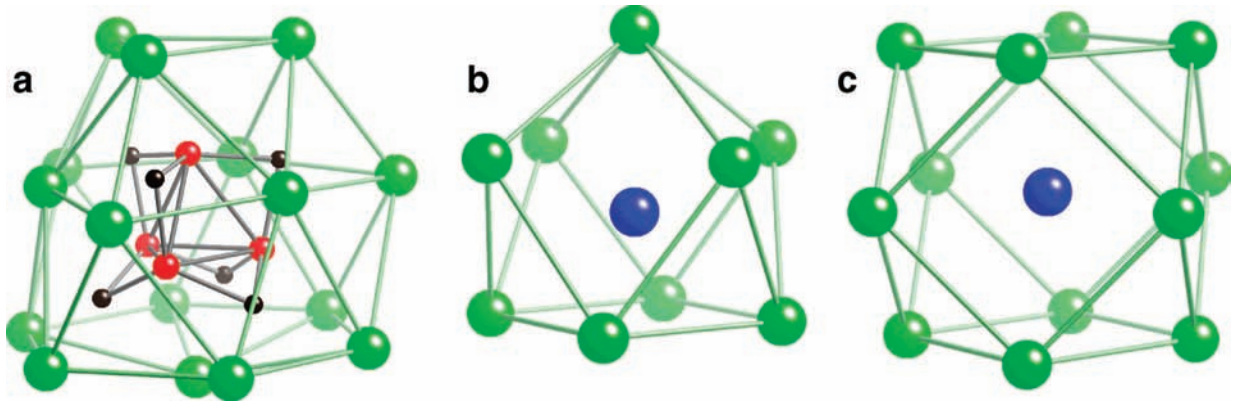

Figure 3. Local coordination environments in $La_{21}Fe_8Sn_7C_{12}$. Green spheres represent lanthanum; the green lines between La sites are drawn to highlight the coordination polyhedra and are not necessarily representative of bonds. (a) The tetrahedral Fe_4C_6 cluster. (b) The capped square antiprism coordination of the Sn1 site. (c) The Sn2 site is weakly coordinated to 12 La sites in a cuboctahedral array.

of an ordered anionic transition metal−carbon building block. The metal-to-carbon ratio of such phases is low, ranging from 1 (YWC_2, $U_5Re_3C_8$) to 2 (YCoC).[19] The other class is the metal-rich carbides, which can be viewed as normal intermetallic phases with interstitial carbon. The occupancy of the carbon in the interstitial sites varies, and the metal-to-carbon ratio is high, ranging from 4 (perovskite analogues such as $ThRu_3C$) to much higher ($Ce_2Ni_{22}C_{3-x}$, $Pr_2Fe_{14}C$).[20] The metal-to-carbon ratio of $La_{21}Fe_8Sn_7C_{12}$ is 3, putting this structure in between the two classifications of metal carbides. However, since the carbon sites are ordered and fully occupied, this compound bears more resemblance to the carbometallates. Accordingly, the Fe_4C_6 cluster can be viewed as an anionic building block surrounded by a La/Sn network, although assigning specific charges to individual atoms is not possible for intermetallic phases with delocalized electrons.

Selected coordination environments in this structure are shown in Figure 3. There are eight Fe_4C_6 clusters per unit cell, comprised of one iron and one carbon site and their symmetry equivalents. The Fe−Fe bond distance is 2.554(4) Å, slightly longer than those of elemental iron (2.48−2.53 Å) but comparable to the bonds seen in iron-rich intermetallics such as $La_2Fe_{14}C$ (2.40−2.58 Å). The carbon atoms cap each edge of the iron tetrahedron, with a Fe−C bond length of 1.915(11) Å. This is shorter than typical distances between iron and isolated carbon atoms in compounds such as $La_2Fe_{14}C$ (2.035 Å) and more comparable to the shorter transition metal−carbon bond distances seen in the carbometallates. These short bonds are theorized to be due to covalent contributions to the bonding in the anionic building blocks in carbometallate compounds.[18]

The Sn1 (24*e*) site is coordinated by nine lanthanum atoms in a square antiprism monocapped axially. A slight aluminum impurity etched from the alumina crucible by the La/Ni flux can be observed mixing on this site in $La_{21}Fe_8M_7C_{12}$ (M = Ge or Te) analogues prepared with long soak times at elevated temperature. The Sn2 (4*a*) site is weakly coordinated by 12 lanthanum atoms in a cuboctahedral array. This site features extremely long bond lengths (Sn2−La1 distance is 3.9891 Å, compared to the normal 3.3−3.6 Å range for La/Sn intermetallics),[17] and in several analogues this atom has a high displacement parameter, which is indicative of the loosely bound atom "rattling" within the cuboctahedron. Similar behavior is observed for heavy atoms in large voids in rare earth stannides such as $Ce_3Rh_4Sn_{13}$, as well as in skutterudite and clathrate thermoelectric materials; this rattling causes scattering of phonons and lowers thermal conductivity, leading to a higher thermoelectric figure of merit.[21−23]

Magnetic Properties. Susceptibility measurements were done on single crystals of $La_{21}Fe_8Sn_7C_{12}$ at several different fields. All data sets show Curie−Weiss behavior at high temperatures, deviations beginning around 100 K, and a cusp near 5 K; see Figure 4a. The effect of trace ferromagnetic impurities (possibly nickel from residual flux coating the crystals) was evident in data collected at low fields, resulting in unusually high moments per iron atom calculated from the Curie−Weiss fit of the inverse susceptibility data.[24] The ferromagnetism of these impurities can be saturated at high fields; data sets collected at 1 T or higher yield $\mu_{eff} = 1.87\ \mu_B$ per iron atom. This μ_{eff} is in the range usually observed for iron in intermetallics (ranging from 1 to 3 μ_B in phases such as $RE_2Fe_{14}B$ and $LaFe_{13-x}Si_x$, for example).[25] The Weiss constant (θ_c) is −185 K. This constant is proportional to the sum of the exchange interactions (J_{ij}) and is usually similar in magnitude to the ordering temperature. A large negative θ_c accompanying a very low ordering temperature is indicative of an antiferromagnetic system that experiences spin frustration.[11,26]

The large antiferromagnetic exchange interactions between iron atoms cause deviations from Curie−Weiss behavior observed below 100 K in the temperature-dependent susceptibility. Below 5 K, a cusp and a separation between ZFC and FC susceptibilities are observed ($T_{SG} = 4$ K, $H = 100$ G), as shown

(19) (a) Jeitschko, W.; Behrens, R. K. *Z. Metallkd.* **1986**, *77*, 788–793. (b) Block, G.; Jeitschko, W. *Monatsh. Chem.* **1987**, *118*, 43–50. (c) Gerss, M. H.; Jeitschko, W. *Z. Naturforsch. B: Chem. Sci.* **1986**, *41*, 946–950.
(20) (a) Wachtmann, K. H.; Moss, M. A.; Hoffmann, R. D.; Jeitschko, W. *J. Alloys Compd.* **1995**, *219*, 279–284. (b) Bodak, O. I.; Marusin, E. P.; Fundamensky, V. S.; Bruskov, V. A. *Kristallografiya* **1982**, *27*, 1098–1101. (c) Gueramian, M.; Bezinge, A.; Yvon, K.; Muller, J. *Solid State Commun.* **1987**, *64*, 639–644.
(21) Niepmann, D.; Pöttgen, R.; Poduska, K. M.; DiSalvo, F. J.; Trill, H.; Mosel, B. D. *Z. Naturforsch. B* **2001**, *56*, 1–8.
(22) Hermann, R.; Jin, R.; Schweika, W.; Grandjean, F.; Mandrus, D.; Sales, B. C.; Long, G. J. *Phys. Rev. Lett.* **2003**, *90*, 135505.
(23) Hermann, R. P.; Schweika, W.; Leupold, O.; Rüffer, R.; Nolas, G. S.; Grandjean, F.; Long, G. J. *Phys. Rev. B* **2005**, *72*, 174301.
(24) Sweet, L. E.; Roy, L. E.; Meng, F.; Hughbanks, T. *J. Am. Chem. Soc.* **2006**, *128*, 10193–10201.
(25) (a) Isnard, O.; Fruchart, D. *J. Alloys Compd.* **1994**, *205*, 1–15. (b) Szytula, A.; Leciejewicz, J. *Handbook of Crystal Structures and Magnetic Properties of Rare Earth Intermetallics*; CRC Press, Inc.: Boca Raton, 1994.
(26) Ramirez, A. P. *Annu. Rev. Mater. Sci.* **1994**, *24*, 453.

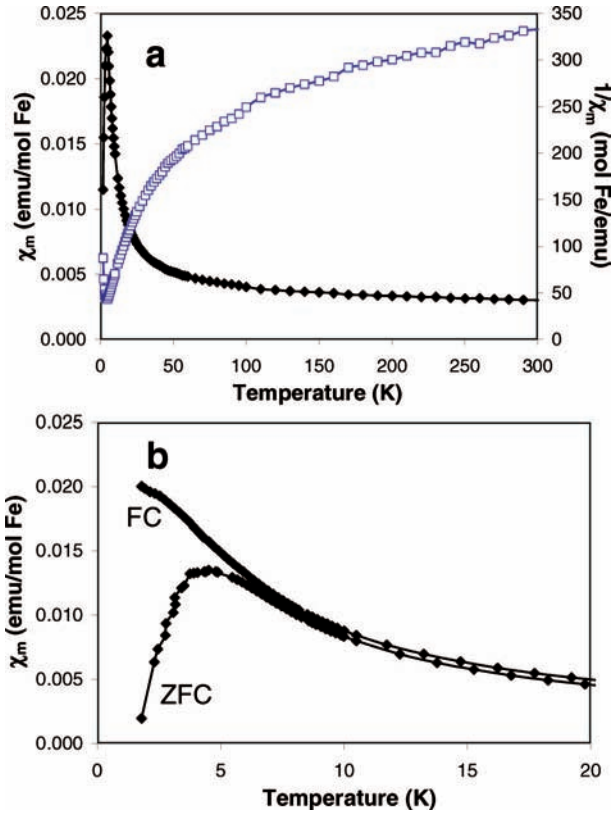

Figure 4. Magnetic susceptibility data for $La_{21}Fe_8Sn_7C_{12}$. (a) Data collected under zero-field-cooled conditions, with a 100 G applied field. Inverse susceptibility data are given in open symbols. (b) Comparison of field-cooled and zero-field-cooled data at low temperature, showing separation at 5 K.

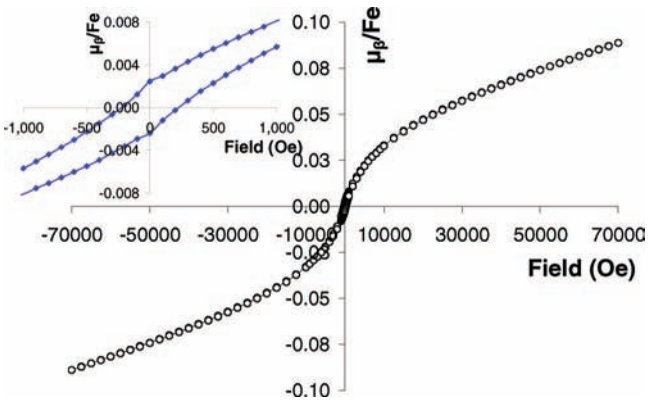

Figure 5. Magnetization data for $La_{21}Fe_8Sn_7C_{12}$ taken at 1.8 K. The inset shows the slight hysteresis observed at low fields.

in Figure 4b. This separation of ZFC and FC susceptibilities indicates a spin glass transition, with the transition shifting to lower temperatures with an increase in applied field. This transition is no longer observed with $H > \sim 750$ G. The magnetization measured as a function of field at 1.8 K, $M(H)$, does not saturate at the highest field of 7 T. A slight hysteresis is observed with a coercivity of ~200 G, shown in Figure 5. The hysteresis and the inability to saturate the sample are consistent with the expected behavior of a spin glass.

The real component of the AC magnetization should exhibit a sharp and frequency-dependent cusp (T_{SG}) in the case of a spin glass. Figure 6 shows the real part (m') of the AC magnetization of $La_{21}Fe_8Sn_7C_{12}$ measured at $\mu_0 H_{dc} = 5$ Oe at

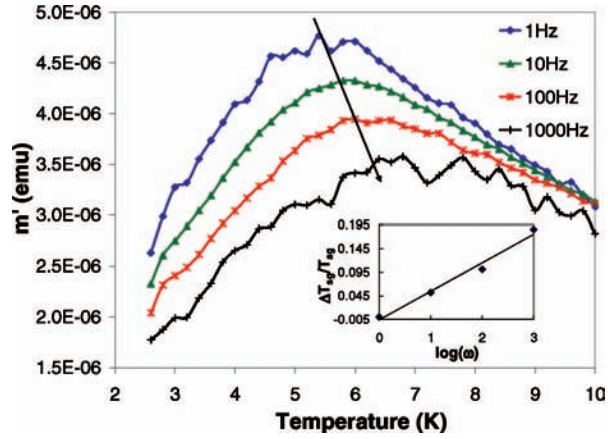

Figure 6. Temperature dependence of the real component of the AC magnetization, m', for $La_{21}Fe_8Sn_7C_{12}$ at different frequencies ω. Inset: Determination of the Mydosh parameter from the variation of spin freezing temperature with frequency.

various frequencies ($\omega = 1$, 10, 100, 1000 Hz). The peak shifts to higher temperatures and decreases in intensity with increasing frequency. A two-point smoothing function of adjacent averaging was applied using Origin graphing software to determine T_{SG}. The Mydosh parameter ($\varphi = \Delta T_{SG}/[T_{SG} \log(\omega)]$) is a quantitative measure of the frequency shift of a spin glass system and was determined to be $\varphi = 0.054$ from the data plotted in Figure 6 (inset). This value is within the expected range (0.004−0.08) for spin glass systems.[27]

The DC and AC magnetization data support spin glass behavior in $La_{21}Fe_8Sn_7C_{12}$. However, there is no detectable disorder between neighboring iron atoms, which contradicts models commonly used to explain the origin of spin glass behavior. Recent theoretical calculations have shown that introduction of weak exchange randomness (disorder) can induce spin freezing and that the disorder strength is proportional to the spin glass transition temperature.[9] The presence of small amounts of aluminum impurity could be a possible source of such weak disorder in the title phase. This is observable in the EDS data of the Te and Ge analogues and is apparent on the 24*e* site in the structure refinement. Small amounts of Al (below the detection limit of EDS, and averaged out in the crystal structure) may be incorporated into all the analogues, causing random strain in the surrounding lanthanum network. Any perturbations in the lanthanum network would generate a slight distortion in the local environment of the iron atom, causing weak disorder in the exchange interactions between neighboring iron atoms and allowing for the formation of the spin glass state. This weak bond disorder between iron atoms is not detectable via X-ray diffraction, since small localized distortions would be averaged out in the crystal structure. Other techniques sensitive to local environments would be needed to detect this disorder. ^{57}Fe and ^{119}Sn Mössbauer studies are currently underway on this compound.

Conclusion

Reaction of iron with other elements in La/Ni flux allows for crystal growth of a variety of compounds with iron clusters, layers, or networks. Growth of large crystals will facilitate more complete studies of the magnetic properties of these iron

(27) Mydosh, J. A. *Spin Glasses: An Experimental Introduction*; Taylor and Francis: London, 1993.

structural moieties. The new intermetallic carbide $La_{21}Fe_8Sn_7C_{12}$ features isolated tetrahedra of iron atoms that exhibit spin frustration. It may be possible to tune this frustration by investigating the other analogues of the structure type, and by purposefully inducing local distortions of the Fe_4 tetrahedra by allowing the deliberate incorporation of impurities into surrounding lattice sites.

Acknowledgment. This research was supported by the FSU Department of Chemistry and Biochemistry, and by the National Science Foundation under grant award numbers DMR-05-47791 and DMR-05-06946. We thank Michael Shatruk and Vasanth Ramachandran for helpful discussions on the magnetism aspects of this work.

Supporting Information Available: Crystallographic data for the $RE_{21}Fe_8M_7C_{12}$ compounds, in the form of CIF files. This material is available free of charge via the Internet at http://pubs.acs.org.

JA809084N